Published in final edited form as:
Int J Pharm. 2014 April 10; 464(0): 185–195. doi:10.1016/j.ijpharm.2014.01.007.

Starch-coated magnetic liposomes as an inhalable carrier for accumulation of fasudil in the pulmonary vasculature

Kamrun Nahar, **Shahriar Absar**, **Brijeshkumar Patel**, and **Fakhrul Ahsan***
Department of Pharmaceutical Sciences, School of Pharmacy, Texas Tech University Health Sciences Center, 1300 Coulter St, Amarillo, TX 79106

Abstract

In this study, we tested the feasibility of magnetic liposomes as a carrier for pulmonary preferential accumulation of fasudil, an investigational drug for the treatment of pulmonary arterial hypertension (PAH). To develop an optimal inhalable formulation, various magnetic liposomes were prepared and characterized for physicochemical properties, storage stability and in vitro release profiles. Select formulations were evaluated for uptake by pulmonary arterial smooth muscle cells (PASMCs)–target cells–using fluorescence microscopy and HPLC. The efficacy of the magnetic liposomes in reducing hyperplasia was tested in 5-HT-induced proliferated PASMCs. The drug absorption profiles upon intratracheal administration were monitored in healthy rats. Optimized spherical liposomes–with mean size of 164 nm, zeta potential of −30 mV and entrapment efficiency of 85%–exhibited an 80% cumulative drug release over 120 hours. Fluorescence microscopic study revealed an enhanced uptake of liposomes by PASMCs under an applied magnetic field: the uptake was 3-fold greater compared with that observed in the absence of magnetic field. PASMC proliferation was reduced by 40% under the influence of the magnetic field. Optimized liposomes appeared to be safe when incubated with PASMCs and bronchial epithelial cells. Compared with plain fasudil, intratracheal magnetic liposomes containing fasudil extended the half-life and area under the curve by 27- and 14-fold, respectively. Magnetic-liposomes could be a viable delivery system for site-specific treatment of PAH.

*Correspondence should be addressed to: Fakhrul Ahsan, Ph.D., Tel.: +1 806 356 4015 x335; Fax: 806 356 4034, fakhrul.ahsan@ttuhsc.edu.

Authors' contribution:
Kamrun Nahar: Ms. Nahar is the primary author of this manuscript. She designed and performed all the experiments, analyzed data and prepared the draft of the manuscript.
Shahriar Absar: Mr. Absar edited the manuscript, wrote the introduction and discussion part. He also performed the microscopic study presented in this manuscript. In addition, Shahriar helped the primary author in performing pharmacokinetic experiment and analyzing the PK parameters.
Brijesh Patel: Mr. Patel taught the primary author several analytical techniques and cell culture related issues. He also was involved in designing cell culture experiments.
Fakhrul Ahsan: Dr. Ahsan is the principal investigator for this work who performed the final editing. Dr. Ahsan is serving as the corresponding author here.

Keywords

Magnetic liposomes; pulmonary delivery; pulmonary arterial hypertension (PAH); lipid-based formulations

1. INTRODUCTION

Over the past several years, magnetic nanoparticles have emerged as a new delivery tool for diagnosis, gene therapy, and targeted pharmacological interventions (Jain et al., 2008; Reiss and Hutten, 2005). In terms of size, these miniaturized particles closely resemble the mammalian cells (10–100μm), viruses (20–450 nm), proteins (5–50 nm) and genes (2nm wide and 10–100nm long); and thus they can move around the body without interrupting physiological functions (Medeiros, 2011). Magnetic nanoparticles (MNPs), that are chemically iron oxide (Fe_3O_4) and known as magnetites, are biodegradable, biocompatible and possess super-paramagnetic properties (Okon et al., 1994). However, one of the major challenges toward using iron oxide based particles as drug delivery vehicles is their tendency to agglomerate and give rise to sediment. In fact, agglomeration of particles in the blood or at any major organ system could be a major safety concern (Medeiros, 2011). Coating of iron oxide particles with surfactants stabilizes against aggregation which then limits the effect of gravitational sedimenation (Shamim et al., 2007; Shubayev et al., 2009). Similarly, coating with dextran confers stability and enhances the dispersibility of particulate systems in the water (Bulte et al., 1999a; Jung and Jacobs, 1995).

To use magnetic particles as drug delivery carriers, drug candidates are often conjugated with coating materials such as dextran, starch, polyethylene glycol and block co-polymers (Alexiou et al., 2000). But coating of particles and conjugation of drug with coating materials can alter MNP surface and physical properties including magnetization, hydrodynamic size, charge and stability. Also, this approach can adversely influence biodistribution (Chouly et al., 1996), weaken drug-particle interaction and enhance drug-particle dissociation (Alexiou et al., 2000; Arias et al., 2008; Kim and Lee, 2001). Magnetic nanoparticles can also be encapsulated into various particulate carriers such as liposomes (Pradhan et al., 2010), polymeric nanoparticles (Li et al., 2011) and magnetic hydrogels (Mitsumata et al., 2012). Of the particulate carriers, liposomes are widely used microscopic spherical vesicles that can encapsulate both lipophilic and hydrophilic drug molecules in their lipid bilayer and aqueous core (Laouini, 2012). Magnetic particles encapsulated in liposomes maintain their magnetic property and exhibit improved pharmacokinetics profiles (Bulte et al., 1999b). They have been used for targeted delivery of drugs to the lung (Plank, 2008), kidney (Salomir et al., 2005), pancreas, brain (Kreuter, 2001), (Schroeder et al., 1998) and colon (Duguet et al., 2006). Because of the presence of super-paramagnetic iron particles in the core, magnetic liposomes accumulate at the disease site and increase drug concentration under the influence of an external magnetic field (Shubayev et al., 2009). In hyperthermic condition, these particles produce fast drug release and increase drug concentration at the organ of interest (Plank, 2008; Shinkai et al., 2001) including the lung.

Indeed, the lungs are the primary site of a number of pathological conditions such as asthma, fibrosis, cancer, infection and pulmonary arterial hypertension (PAH). Of the lung diseases,

PAH is a rare and progressive pulmonary vascular disease; proliferation and contraction of pulmonary arterial smooth muscle cells are chief pathological alterations that occurs in PAH. Thus, it reduces pulmonary arterial lumen diameter, increases pulmonary vascular resistance, decreases reactivity of the vascular bed and eventually increases pulmonary arterial pressure (Mucke, 2008). Currently, endothelin receptor antagonists (e.g. ambrisentan and bosentan), prostacyclin analogs (e.g. epoprostenol, treprostinil and iloprost), phosphodiesterase-5 inhibitors (sildenafil), anticoagulants, calcium channel blockers, oxygen and nitric oxide (NO) are used for the treatment of PAH. However, these therapeutic agents are of short-lived and necessitate indwelling central catheters, dose escalation (Mucke, 2008), continuous dosing of longer acting prostacyclin analogs (Chattaraj, 2002) and frequent administration of nebulized formulations (Baker and Hockman, 2005). Furthermore, since available therapeutic agents lack pulmonary vascular selectivity (Nagaoka et al., 2005), peripheral vasodilatation and consequent systemic hypotension is common in PAH patients. Recent development in PAH therapy suggest that Rho kinase, a downstream effector of GTPase Rho, plays major roles in the pathogenesis of PAH. This enzyme is involved in smooth muscle contraction, cell adhesion, migration, cell growth and reorganization of actin cytoskeleton (Amano et al., 1997; Kimura et al., 1996). Thus, Rho-kinase inhibitors have come up as a new class of therapeutic agent for PAH. We and others have shown that fasudil, a Rho-kinase inhibitor, reduces pulmonary arterial pressure in PAH animals and human patients (Gupta et al., 2013; Oka et al., 2007). But lack of pulmonary selectivity remains to be a problem for this drug too.

To enhance pulmonary selectivity, we propose to develop a magnetic liposomal system that can be administered via the pulmonary route and that will help accumulate the drug in the pulmonary vasculature by means of an applied magnetic force. The proposed formulation is likely to release the drug slowly over a long period of time and produce sustained localized pulmonary arterial vasodilation. Toward this end, we have developed an MNP-based liposomal formulation of fasudil. We have encapsulated various iron oxide particles and fasudil in the liposomes and evaluated the feasibility of the resulting particles for inhalational delivery and assessed the influence of the magnetic field on the uptake of the particles by pulmonary arterial smooth muscles cells (PASMC). We have also studied particles' influence on proliferation of PASMC. Finally, we have monitored the pharmacokinetics after intratracheal administration and evaluated the safety with PASMC and Calu-3 bronchial epithelial cells.

2. MATERIALS AND METHODS

2.1. Materials

Phospholipids were purchased from Avanti Polar Lipids Inc. (Alabaster, AL). All other chemicals were purchased from Fisher Scientific (Pittsburgh, PA) or Sigma Aldrich Inc. (St Louis, MO). Anionic (Ferro Tec EMG 707) and cationic (Ferro Tec EMG 607) magnetic nanoparticles with an average particle size of 10 nm and saturation magnetization of 11 militesla (mT) were provided by Ferrotec Inc. (Bedford, NH) without any charge. Fluid Mag-HEAS, a commercially available ferrofluid containing Fe_3O_4 particles, was a generous gift from Chemicell GmbH (Berlin, Germany). The core size of these particles was 35 nm

and is composed of multiple 8–10 nm crystals of Fe_3O_4. The final hydrodynamic diameter due to starch coating was 80 nm. In terms of magnetic properties, these particles had zero coercivity, zero remanence, unsaturation at 30 kOe) (Pradhan et al., 2010). A 96 wells permanent magnetic plate, made of neodymium-iron-boron (NdFeB) with a magnetic strength of 280 mT was purchased from Chemicell GmbH (Berlin, Germany). All chemicals were of analytical grades and used without further purification. Pulmonary arterial smooth muscle cells were supplied by Dr. Eva Nozik-Grayck of University of Colorado (Denver, Colorado) and cell media was purchased from ATCC (Manassas, VA). Extruder and polycarbonate membranes were from Avestin Inc. (Ontario, Canada).

2.2. Preparation of magnetic liposomes of fasudil

Various magnetic liposomes were prepared by varying lipid-to-drug ratio, lipid composition, type of magnetic particles, and screened for optimal formulations (Table 1). Lipids used were 1,2-dipalmitoyl-sn-glycero-3-phosphocholine (DPPC), cholesterol and 1,2 disteroyl-sn-glycero-3-phosphoethanolamine-N-[methoxy (polyethylene glycol)-2000] (DSPE-PEG_{2000}). Three different iron oxide particles–anionic, cationic and starch coated–were used to prepare various formulations. Liposomes were prepared by solvent evaporation-extrusion method. Briefly, lipids were dissolved at different molar ratios in 2 mL organic solvent composed of chloroform and methanol in a round-bottom flask which was placed under vacuum in a water bath at 45°C using a Buchi R-114 Rotavapor (Buchi Laboratories AG, Postfach, Switzerland) to form a thin lipid film. For a complete removal of the organic solvent, the film was kept under vacuum for additional 2 hours after film formation. The dried lipid film was then rehydrated with 250 mM ammonium sulfate (pH 5.4) containing varying amounts of various magnetic particles. Crude liposomes thus obtained were sonicated for an hour to prepare multilamellar vesicles and then extruded sequentially through 400 and 200 nm polycarbonate membranes to get unilamellar vesicles. As shown in Table 1, for formulations F-1 and F-2, anionic and cationic magnetic particles were encapsulated into liposomes and for formulations F-3 to F-17, hydroxyethylstarch coated magnetites were encapsulated. Un-entrapped magnetic particles were removed by centrifugation and the external buffer was replaced with phosphate buffered saline (PBS) at pH 7.4 using a PD-10 column (sephadex-25, GE Healthcare, Piscataway, NJ) to create a gradient of ammonium sulfate between the external and internal buffers. Liposomes were then incubated with 10 mg of fasudil dissolved in the external buffer for two hours at 65°C. Un-encapsulated fasudil was removed with a PD-10 column.

Optimization of process parameters—Magnetic formulations were optimized for various process parameters including incubation buffer and time, number of extrusion cycles and centrifugal speeds. To maximize fasudil entrapment in the liposomes, we have used three external buffers (PBS, HEPES and Tris at pH of 7.4) and ammonium sulfate solution (pH 5.4) as the only internal buffer. Similarly, incubation time was optimized by incubating the drug with extruded liposomes for 20, 30, 60, 120, 135 and 150 minutes. Furthermore, the optimum extrusion cycle was identified by extruding the liposomal preparations 5, 9, 15 and 21 times through 200 nm polycarbonate membranes. Separation of unentrapped magnetites from the nanoparticles is a critical step in preparing magnetic particle based drug delivery

systems, and thus, centrifugation speed was optimized by centrifuging the fasudil loaded liposomes at 1000, 2000, 4000, 6000, 8000 and 10000×g.

2.3. Physicochemical characterization of magnetic liposomes

Magnetic liposomes were characterized for morphology, hydrodynamic diameter, polydispersity index (PDI), zeta potential and entrapment efficiency. The morphology was studied in a transmission electron microscope (TEM) (Hitachi H-7650, Hitachi High Technologies America, Inc., Pleasanton, CA). The samples were not stained for this experiment as the liposomes had magnetic nanoparticles that could be observed owing to higher electron density. For size measurement, 20 µl liposomes were taken into an Eppendorf® tube and diluted with PBS. To measure zeta potential, the samples were diluted with water to avoid ionic interferences. Both mean size based on % intensity and zeta potential was measured in a Nano ZS90 Zetasizer (Malvern® Instruments Ltd., Worcestershire, UK). For each characterization study, each formulation was prepared thrice (n = 3) with the same lipid, drug and magnetite composition. Various parameters of each formulation were then measured three times. PDI was calculated using an algorithm described in ISO 22412:2008 and ISO 13321: 1996).

Fasudil concentrations in the liposomes were determined by a UV spectrophotometer (HP 8453A, Olis Inc., Hayward, CA) by lysis of liposome lipid layer with methanol. Briefly, 50 µl of liposomes were taken into an Eppendorf® tube containing 950 µl methanol and sonicated for 15 minutes. This was then centrifuged at 17000xg (Legend Micro 17R, Thermo Scientific, Waltham, MA)) for 15 minutes and absorbance of the clear supernatant was taken at 320 nm. The fasudil encapsulation efficiency was calculated using the following formula: $L/T \times 100$ (Where L is *the* amount of fasudil in the liposome, *T* is the total amount of fasudil added).

Determination of magnetite content—The amount of magnetic particles to be used in the formulation was optimized for maximum drug encapsulation in the liposomes. Formulations were prepared with varying amounts of magnetic particles, i.e. 2.5, 5, 10 and 20 mg but the total lipid quantity was 50 µmole (F-10, F-15, F-16 and F-17). Following removal of un-entrapped magnetic particles by centrifugation at 6000xg, iron quantity was determined by a colorimetric method using 1, 10 ortho-phenanthroline (Pradhan et al., 2010). Fasudil content in each liposomal formulation was determined as described above.

Stability of liposomes—The stability of the formulations was evaluated by monitoring the size of F-1, F-2, F-4 and F-10 formulations for over a month at a storage temperature of 4°C and 25°C. To determine if the drug is leaching out of the vesicles with time, the entrapment efficiency of F-10 formulations was also monitored periodically for a month. Similarly, zeta potential of F-10 formulations was also monitored throughout the storage period. Since these magnetic liposomes are intended to be administered via the intratracheal route using a MicroSprayer™ (PennCentury®, Inc., Philadelphia, PA), the stability of the vesicles upon aerosolization was also assessed. Briefly, F-10 liposomal preparations were placed in a MicroSprayer™, aerosolized and collected for characterization of size, zeta potential and entrapment efficiency (Gupta et al., 2013) as described above. For

determination of fasudil content, aerosolized liposomes were diluted with PBS and un-encapsulated fasudil (if any) was separated from the liposomes by centrifugal filtration using an Amicon Ultra® tube (MWCO-3000, Millipore Inc., Billerica, Massachusetts, USA) and the drug concentration was determined as described above.

2.4. Magnetization study

This experiment was performed to evaluate magnetic property of the optimized formulation, F-10, in response to an applied magnetic field. Briefly, 20 μl of fluorescently labeled magnetic liposomal formulation was diluted to 1 mL with PBS. A drop of the diluted formulation was placed on a glass slide and positioned on the 96-weel permanent magnetic plate for 20 minutes. Movement of the formulation along the direction of applied filed was determined by taking fluorescent images at the beginning and after 20 minutes at 40X magnification.

2.5. In-vitro release study

The release profiles were determined according to our previously published method (Gupta et al., 2013). To evaluate the influence of lipid composition and iron content on the release profiles, we have used F-9, F-10, F-11, F-15 and F-16 (Table 1) in this study. Briefly, 500 μl of liposomal suspension was placed in a dialysis Cassettes (Slide-A-Lyzer, 3500 MWCO, 0.1–0.5 ml, Thermo-Scientific, Waltham, MA) suspended in a beaker containing 50 ml of PBS, pH 7.4 at 37°C. An aliquot of the sample (1 mL) was collected for various time points and replaced with the same volume of fresh media. The drug release was evaluated by disrupting the liposomes with 1% triton X-100 at time zero and drug concentration was determined using a UV spectrophotometer. Percent fasudil released at different time points was determined using the following equation: % release = $100 \times (F_t - F_0)/(F_{100} - F_0)$, where F_t and F_0 are the concentrations at time ‘t’ and time ‘0’, respectively. F_{100} represents 100% fasudil concentration from the liposomes.

Cell viability study—The compatibility of the fasudil, plain liposome (F-18) and magnetic liposomes (F-10) were studied by determining the viability of bronchial epithelial cells (Calu-3) and pulmonary arterial smooth muscle cells (PASMC) using a MTT assay (Patel et al., 2012). Briefly, 50,000 PASMC and Calu-3 cells were seeded on 96 wells flat bottom plates and kept overnight for cells to attach. Next day, plain fasudil, plain liposomes (F-18) and magnetic liposomes (F-10) containing 25, 50, 100 or 250 μM fasudil was added to 96-well plates, placed on a permanent magnetic plate, and incubated for four hours at 37°C. The culture media was then replaced with 100 μl of fresh media containing 0.5 mg/ml MTT solution and incubated for another four hours. After removing the MTT solution, the crystalline precipitate was dissolved in dimethyl sulfoxide (DMSO) and absorbance was measured at 570 nm. The percent of viable cells were calculated from the following equation: % of viable cells = $(A_{\text{treated}} - A_{MTT})/(A_{\text{control}} - A_{MTT}) \times 100$.

2.7. Cellular uptake study

Both qualitative and quantitative studies were performed to evaluate cellular uptake. For qualitative study, the uptake of F-10 formulation by rat PASMCs was tested under the influence of a magnetic field using a fluorescence microscope (Pradhan et al., 2010). In

short, rat PASMCs were cultured in 75 cm^2 flask in 10% FBS, penicillin/streptomycin and glutamine containing DMEM F-12 media (ATCC, Manassas, VA) at 37°C in 5% CO2 atmosphere. Cells (10,000) were seeded on glass cover slip and kept overnight to attach on the surface. The cells were then incubated with fluorescent labeled (rhodamine B) magnetic liposomes for two hours with or without the influence of magnetic field. For studying the influence of magnetic fields, slides were placed over a 96-well magnetic plate as discussed above. After washing three times with saline, the cells were fixed with 4% freshly prepared paraformaldehyde solution and stained with DAPI (4′,6-Diamidino-2-Phenylindole, Dihydrochloride), Carlsbad, CA. The cells were then viewed under a fluorescent microscope (IX-81, Olympus, Center Valley, PA).

To quantify cellular uptake, 5×10^5 cells were separately seeded in 12 wells plate and kept overnight at 37°C. The cells were then incubated for two hours with 250 μM of fasudil or equivalent amount of magnetic liposomes in the presence or absence of the magnetic field. Like above studies, for magnetic influence, cells placed on a 96-well magnetic plate. After washing thrice with ice cold PBS, the cells were trypsinized and collected by centrifugation followed by dispersion again in ice cold PBS. The cells were then lysed with 1% triton X-100 and analyzed for fasudil content by HPLC. The amount of fasudil was determined from the standard curve, while number of cells was determined indirectly upon quantification of total protein by bicinchonic acid (BCA) protein assay (Pierce, Rockford, IL).

2.8. Cell proliferation assay

The effect of fasudil loaded magnetic liposomes (F-10) in attenuating proliferation of PASMCs was evaluated by MTT assay (Chen et al., 2009). Cells were seeded on 96 wells plate and kept overnight to get attached on the well surface. Next day, the cells were incubated with 25, 50 and 100 μM plain fasudil or F-10 formulations containing equivalent amount of fasudil for 24 h. The incubation was performed in the presence or absence of the magnet to evaluate the relative efficacy in inhibiting cell proliferation. Cells were then stimulated with 2 μM 5-HT for 24 hours followed by incubation with 100 μl MTT reagent at 37°C for 4 hours. The precipitated formazan crystals were dissolved in DMSO and the absorbance was read at 570 nm.

2.9. Pulmonary absorption studies in rats

The in vivo absorption studies were carried out in healthy Sprague Dawley rats. Briefly, rats (250–300g) were divided into three groups: (i) fasudil intravenous, (ii) fasudil intratracheal, and (iii) magnetic liposome (F-10) intratracheal. The formulation for in vivo studies was selected based on stability, drug loading and in vitro release profile. Rats were anesthetized by an intramuscular injection of a cocktail of ketamine (90 mg/Kg) and xylazine (10 mg/Kg). After exposing the trachea using a laryngoscope, 6 mg fasudil or formulation containing equivalent amount of fasudil were administered by a Microsprayer® (Model IA-1B; Penn Century Inc., Philadelphia, PA). Blood samples were collected at various time points from the tip of the tail in heparin coated Eppendorff® tubes and were placed on an ice bath. The plasma was separated by centrifuging the blood at 2400×g for 10 min at 4°C and stored at −20°C until further analysis. For sample analysis, 100 μl of plasma was taken in an

Eppendorff® tube onto which 30 μl of 3% Triton X-100 and 170 μl of acetonitrile were added, vortexed for few minutes and centrifuged at 17000×g for 15 min at 4°C. Clear supernatant was injected into the HPLC (Varian Prostar 320, Walnut Creek, CA). Chromatographic condition was C18X 250 mm × 4.5 mm, particle size 5 μM, mobile phase 0.02 mM phosphate buffer: acetonitrile = 68:32; flow rate: 1ml/min; wave length 225 nm and injection volume 100 μl. Drug concentration was calculated from a standard curve.

Data Analysis—The data are presented as mean±SD and were analyzed by ANOVA followed by a *Post hoc* analysis using Tukey's comparison (GraphPad Prism, version 5.0, GraphPad Software, San Diego, CA). To calculate pharmacokinetic parameters, standard non-compartmental analysis Phoenix WinNonlin® (Sunnyvale, CA) was performed. p value less than 0.05 was considered statistically significant.

3. RESULTS

3.1. Physical characterization

Magnetic liposomes were round shaped (Fig. 1A) and magnetic particles were present both in the core and surface of the liposomes (Fig. 1B). The diameters of the liposomal particles were between 119 and 199 nm (Table 1). Entrapment of iron particles appeared to contribute to the size of the liposomes based on the observation that liposomes containing iron particles were larger compared to plain liposome. Another important parameter, i.e. poly dispersity index (PDI) that is a dimentionless number that measures the breadth of size distribution, which indicates whether a colloidal system is monodisperse or heterodisperse. PDI values varies from 0.05 to 1.0; a PDI of 1.0 indicates a very broad size distribution.PDIs of most of the formulations were less than 0.2 (Table 1), which indicates a monodispersed colloidal system (Kim et al, 2009). The PDI of pegylated liposomes was smaller than non-pegylated liposomes, which could be attributed to the presence of pegylated lipid in the formulations that perhaps contributed to the steric hindrance via the hydrophilic groups of PEG (Bai and Ahsan, 2010) and that might be also the reason for improved colloidal stability with smaller PDI values. All liposomes, but F-2, were negatively charged (−6 to −40 mV in Table 1), pegylated liposomes with the highest negative value. This negative charge might have stemmed from the zwitterionic phosphatidylcholine used in liposomes. These phospholipids carry a net negative charge that can contribute to the negative zeta potential of liposomal formulations (Natarajan et al., 2011). The higher negative values observed for pegylated liposomes can come from the carbamate linkage–which is reported to give rise to a net negative charge on the phosphate moiety at physiological pH–between PEG and DSPE (Absar et al., 2013). The positive charge of F-2 is from cationic magnetite used in the formulations. Nevertheless, most of the formulations exhibited optimal charge characteristic, suggesting colloidal stability.

Entrapment of fasudil was evaluated after both passive and remote loading of the drug. Passive loading method was used for anionic and cationic magnetites as these magnetites forms aggregates at concentrated ammonium sulfate solution (data not shown). The passive loading method in case of F-1 and F-2 demonstrated fasudil entrapment of 4.5 to 5.5% (Table 1). But active loading method was used for starch-coated magnetites (F-3 to F-17) using ammonium sulfate gradient: the entrapment was ~ 92% (Table 1). When total lipid

quantity was increased from 25 μmol to 50 μmol, the entrapment efficiency was increased from 55% to 83%. However, increase in the entrapment upon further increase in lipid quantity (75 μmol) was negligible. At similar lipid composition, pegylated liposomes exhibited higher entrapment compared to that of non-pegylated liposomes, which could be due to increased hydrophiliciy of pegylated lipids. It is possible that a fraction of hydrophilic fasudil got entangled within the pegylated arms of liposomes (Bai and Ahsan, 2010). The effect of magnetite amount on the entrapment efficiency was measured to optimize the formulations. An increase in the magnetite amount resulted in an increase in iron content in liposomes (Fig. 2). Based on these data, 100 to 200 μg of magnetite/μmol of lipid was chosen as an optimum condition.

3.2. Stability of the liposomes

The stability of magnetic liposomes at two different storage temperatures, 4°C and 25°C, was evaluated in terms of size, zeta potential and entrapment efficiency. Non-pegylated liposomes (F-1, F-2 and F-4) prepared with anionic, cationic and starch coated magnetites were not stable even for 7 days at 4°C (Fig. 3). Within a week, liposomes were aggregated as evident by an increase in size of the liposomes along with formation of sediments. However, pegylated liposomes (F-10) were stable for more than 28 days at 4°C (Fig. 3). Enhanced stability of F-10 can be attributed to the steric hindrance conferred by PEG (Bai and Ahsan, 2010). Stable F-10 was further characterized for its ability to retain the drug within the vesicles throughout the storage period. Liposomes stored at 4°C did not show any change in the amount of entrapped drug; but around 30% drug was lost when stored at 25° for 4 weeks (Fig. 4A). Thus at higher temperature, the drug was leaching out of the vesicles which is consistent with earlier observations that at higher temperature the fluidity and permeability of phospholipid bilayer increases (Bai and Ahsan, 2010). Furthermore, no change in the zeta potential was observed during the storage period, confirming the colloidal stability of F-10 formulations (4B). Since the formulations are intended to be administered via the pulmonary route, their stability following nebulization is also important. No significant change in the size, zeta potential and entrapment efficiency (Table 2) of the liposomes was observed following nebulization of optimized formulation (F-10). These results indicate that the formulations were stable to withstand the physical force applied during nebulization.

3.3. Influence of buffer type, extrusion, incubation time and centrifugal speed

Of the three different external media (Tris, HEPES and PBS buffer) used to entrap fasudil by active loading method, the highest entrapment (87%) was observed with PBS, whereas with Tris and HEPES buffer, fasudil entrapment was 48% and 55%, respectively (Fig. 5A). Fasudil entrapment by this method was performed by ammonium sulfate gradient that keeps ammonium sulfate in the liposome core. Thus when fasudil becomes ionized and gets trapped when it enters the liposome core from the external media. We reasoned that since Tris and HEPES buffer contain ammonium and sulfate ions, respectively, these may contribute to the formation of a complex with fasudil in the external buffer and thereby interfere with the development of ammonium sulfate gradient, resulting in low drug entrapment (Cern et al., 2012). As phosphate buffer is free of sulfate ions, it produced maximum drug entrapment. In case of optimizing the extrusion cycle, when extrusion cycle

was increased from five to fifteen, liposomes size decreased from 198 to 167 nm, respectively (Fig. 5B). However, increasing extrusion cycle from 15 to 20 did not result in much difference in size. The PDI of the liposomes, following each extrusion cycle, was around 0.114 or less, indicating a monodispersed colloidal system.

Further, for maximum drug entrapment, the incubation time of the liposomes (F-10) with the external buffer containing the drug was also optimized. Increasing the incubation time from 20 to 120 minutes, the entrapment efficiency was increased from 10.5±0.5 % to 81±2% (Fig. 5C). However, further increase in incubation time (>120 minutes), increased the entrapment only by 4–5%. Next, the centrifugal condition for purification of unentrapped iron from the magnetic liposomes was optimized. With the increase in rotational force (from 1000 to 6000xg), an increase in the sediment volume was observed (Fig. 5D). However, liposomes and magnetites were separated into two layers at 10000xg, indicating that high rotational speed is not suitable for an optimal separation.

3.4. In vitro release profile

Fasudil was released at a controlled fashion for 5 days and drug release was significantly influenced by the lipid composition. A decrease in cholesterol from 40% to 20% increased the cumulative release from 60% to 82%, respectively (Fig: 6). While plain drug was instantaneously released, the release rate constant, calculated using Higuchi equation, for F-10 formulation was 0.2663 ± 0.019 mg/$h^{1/2}$, suggesting a slowing in drug release.

3.5. Cell viability study

The viability of Calu-3 cells was not affected neither with the increasing concentration of plain fasudil (from 25 μM to 250 μM) nor with equivalent concentration of plain and magnetic fasudil liposome (Fig. 7A). The viability study with PASMC also demonstrated a similar safety profile as observed with Calu-3 cells (Fig. 7B).

3.6. Magnetization of fasudil-encapsulated magnetic liposomes

A central feature of the proposed formulation is their ability to respond to a magnetic field, which was tested using rhodamine-labled magnetic formulations (F-10) under an applied magnetic field. When fluorescent liposomes were monitored in the absence of the magnetic field, a homogenous distribution throughout the glass cover slide was observed (Fig. 8A). Upon application of 280 mT magnetic force, the liposomes rapidly migrated towards the magnet (Fig. 8B); after 10 to 15 minutes, liposome sample was accumulated on top of the magnetic plate and no fluorescent magnetic liposomes were observed outside the magnetic zone (Fig. 8C). Thus, these data clearly demonstrate that formulations are attracted to the magnetic field, the chief feature for magnetic targeting strategy.

3.7. Uptake of the formulations by PASM cells

The site of action of fasudil is the pulmonary arterial smooth muscle cells and the target receptor, Rho-kinase, is expressed on this cell surface. When DAPI stained PASMC cells were incubated for two hours with fluorescent magnetic liposomes (F-10) without magnetic field, some of the liposomes were taken up by the cells (Fig. 9A). However, when the incubation was performed under an applied magnetic field, a significantly higher uptake was

observed. This qualitative observation was further confirmed by a quantitative estimation of fasudil inside the cells using an HPLC assay. The magnetic field had no influence on the uptake of either plain fasudil or liposomes without any magnetic field (Fig. 10). However, under a applied magnetic field, the uptake was increased by 3-fold for the magnetic liposomes, compared with plain liposomes or magnetic liposomes without magnetic field, indicating that magnetic field can facilitate the uptake of fasudil into the pulmonary smooth muscle.

Effect of fasudil-encapsulated magnetic liposome on cell proliferation—A characteristic feature of PAH is the proliferation of smooth muscle cells (McLaughlin and McGoon, 2006). Thus, the effect of the magnetic formulation in attenuating cell proliferation was tested in 5-HT induced PASMC cells. Treatment with plain fasudil attenuates 5-HT induced proliferation PASM cells (Fig. 11), although such attenuation of proliferation was not prominent for magnetic liposomes in the absence of magnetic field. When a magnetic field was applied, a remarkable reduction of cell proliferation was observed which was similar to that of plain fasudil. This observation further confirms our finding presented above (Fig. 8) that magnetic field force the liposomes to be taken up by the cells, which attenuates proliferation of cells (Liu et al., 2011).

3.8. In vivo absorption profile

In vivo absorption study of the optimized magnetic liposomes (F-10) was evaluated in healthy rats following intratracheal administration. The plasma half-life of plain fasudil after IV administration was 19.35±4.88 min, which was increased up to 35.51±5.12 min following IT administration, a 1.8-fold increase in the half-life. However, intratracheal administration of pegylated magnetic liposomes demonstrated a 27-fold increase in drug plasma half-life (Fig. 12). The C_{max} of fasudil, administered via IV, is greater than that via IT. Moreover, the AUC of magnetic liposomes was increased by 14-fold compared with that of plain drug (Table 4). Similarly, plain drug was absorbed instantaneously, but the absorption rate constant of the intratracheally administered magnetic liposomes was 0.083 min^{-1}. The larger AUC values from IT liposomes compared with that of plain IV fasudil is due to the fact that liposomes were lyzed for quantitating the drug concentration in the blood. Thus, circulating intact liposomes containing the drug was taken into account to quantify the drug level in the blood. However, the metabolic instability of the liposomes in the lung is very unlikely because drug concentration in the plasma was imperceptively low when blood sample was analyzed without disrupting the liposomes. The increase in the half-life of fasudil from the liposomal formulation may be attributed to the presence of PEG that creates a hydration layer in the surface of the liposomes thus particles can escape uptake by macrophages and clearance by reticular endothelial systems (Lian and Ho, 2001).

4. DISCUSSION

We and others have demonstrated the feasibility of liposomal formulation for intratracheal delivery of hydrophilic and hydrophobic small and/or macromolecules (Bai and Ahsan, 2010; Gupta and Ahsan, 2011; Gupta et al., 2013). It is now established that intratracheal administration of liposome can offer relative site-specificity and avoid off-target effects.

However, a fraction of the intratracheally administered liposomes with a size range of 100 to 200 nm may reach the blood circulation (Conhaim et al., 1988), which can give rise to systemic effect. To avoid such situation, we have proposed magnetic formulation that can be kept in the lung region by an externally controlled magnetic field so that all the particles remain at the site of action throughout the treatment period. Since PAH is a disease of terminal pulmonary vasculature, a delivery system that accumulates in pulmonary bronchioles and releases drug in a controlled fashion might minimize the shortcomings of current anti-PAH medications. With that in mind, the magnetic formulations of fasudil were prepared and characterized. The size, zeta potential, PDI and entrapment efficiency data demonstrated the feasibility of these formulations for pulmonary delivery. During preparation of liposomes, anionic and cationic magnetites were not tested further because they were not suitable for active loading, the most efficient entrapment method for fasudil (Ishida et al., 2002). Furthermore, the incubation temperature during active loading was selected to be 65°C. The phase transition temperature of the major lipid component, DPPC, of the liposomal formulation is 41°C. It is reported that incorporation of 4 mol% DSPE-PEG_{2000} increases phase transition temperature by 1°C (Needham et al., 2013). But in our formulation, we have used <5mol% of DSPE-PEG_{2000} which might have not influenced phase transition temperature of the lipid. Use of >20 mole% cholesterol can reduce the permeability of the phospholipid bilayer, but may not retard the entry of fasudil into liposome core when incubated at 65°C as reported by Gupta et al (Gupta et al., 2013). In fact, when incubated at temperatures higher than phase transition temperatures of lipids (65°C in this case), amphipathic and unprotonated bases become trapped within liposome core (Uster et al., 1996). For localized action mediated by external magnetic field, the drug must not release from the formulation, as that increases the possibility of producing vasodilatory effect elsewhere other than the target site. The in vitro release study demonstrated that fasudil is released in a controlled fashion over 5-days, suggesting the possibility of long-term lung-specific action of the drug.

Iron particles can be toxic to cells if given at a higher concentration and thus we have used starch-coated magnetites which are biocompatible and biodegradable (Gupta and Gupta, 2005), Iron particles can also be taken up by the alveolar macrophages. However, since the particles are in the cores of pegylated liposomes, we anticipate minimum macrophage uptake for our formulations (Patel et al., 2012). Furthermore, it is reported that particles within a size range of <1μ can escape macrophage uptake (Geiser, 2010) and favors the formulation to be used via pulmonary route.

Since the formulations are expected to act on PASMC to exert their activity, we studied the uptake profiles in the presence or absence of magnetic field. The uptake of magnetic liposomes under the magnetic field was similar to that of plain drug. Similarly, the proliferation activity under magnetic field demonstrated almost equal activity when compared with plain fasudil. Similar to in vitro release profiles, the absorption was instantaneous for plain drug but drug absorption rate went down for liposomal formulations (Figs. 6 and 12). The rationale of using magnetic liposomes, despite similar cellular uptake and in vitro activity, is that plain fasudil causes systemic vasodilation and consequent hypotension, whereas the proposed magnetic particles are designed to be accumulated at the diseased site. A delivery strategy that produces similar effect at the site of action is expected

to result in significant improvement in therapeutic efficacy and safety. This, together with the in vitro behavior under an applied magnetic field, demonstrates the feasibility of using this delivery system for prolonged vasodilation of pulmonary vasculature that occurs during PAH.

5. CONCLUSIONS

This study demonstrates the feasibility of magnetic liposomes as carriers for localized delivery of fasudil, an investigational anti-PAH drug, into the lungs. Indeed, favorable physicochemical properties, release kinetics, enhanced cellular uptake and anti-proliferative effect and extended half-life established the viability of magnetic liposomes for inhalational delivery. However, the efficacy of the formulations in reducing pulmonary arterial pressure and ameliorating pathogenesis in biochemical and cellular levels should be evaluated in an animal model of pulmonary arterial hypertension

Acknowledgments

We thank Drs. Hussaini Qhattal and Vinay Kumar of TTUHSC, Amarillo, TX, for their help in liposome preparation and fluorescent microscopic study. We also acknowledge Mr. Charles Linch at the Department of Medical Photography and Electron Microscopy, TTUHSC, Lubbock, TX, for his help with the transmission electron microscopy experiments. This work was supported in part by an American Recovery and Reinvestment Act Fund, NIH 1R15HL103431.

ABBREVIATIONS

5-HT	5-Hydroxy tryptamine
AUC	Area under the curve
BCA	Bicinchonic acid
DAPI	4′,6-diamidino-2-phenylindole
DMEM	Dulbecco’s modified eagle medium
DMSO	Dimethyl sulfoxide
DPPC	1,2-dipalmitoyl-sn-glycero-3-phosphocholine
DSPE-PEG$_{2000}$	1,2 disteroyl-sn-glycero-3-phosphoethanolamine-N-[methoxy (polyethylene glycol)-2000]
FBS	Fetal bovine serum
HPLC	High performance liquid chromatography
MNP	Magnetic nanoparticles
MRI	Magnetic resonance imaging
MTT	(3-(4,5-Dimethylthiazol-2-yl)-2,5-diphenyltetrazolium bromide
PAH	Pulmonary arterial hypertension
PASMC	Pulmonary arterial smooth muscle cells
PBS	Phosphate buffered saline

PDI	Polydispersity index
TEM	Transmission electron microscopy

References

Absar S, Nahar K, Kwon YM, Ahsan F. Thrombus-targeted nanocarrier attenuates bleeding complications associated with conventional thrombolytic therapy. Pharm Res. 2013; 30:1663–1676. [PubMed: 23468049]

Alexiou C, Arnold W, Klein RJ, Parak FG, Hulin P, Bergemann C, Erhardt W, Wagenpfeil S, Lubbe AS. Locoregional cancer treatment with magnetic drug targeting. Cancer Res. 2000; 60:6641–6648. [PubMed: 11118047]

Amano M, Chihara K, Kimura K, Fukata Y, Nakamura N, Matsuura Y, Kaibuchi K. Formation of actin stress fibers and focal adhesions enhanced by Rho-kinase. Science. 1997; 275:1308–1311. [PubMed: 9036856]

Arias JL, Ruiz MA, Gallardo V, Delgado AV. Tegafur loading and release properties of magnetite/poly(alkylcyanoacrylate) (core/shell) nanoparticles. J Control Release. 2008; 125:50–58. [PubMed: 17949844]

Bai S, Ahsan F. Inhalable liposomes of low molecular weight heparin for the treatment of venous thromboembolism. J Pharm Sci. 2010; 99:4554–4564. [PubMed: 20845454]

Baker SE, Hockman RH. Inhaled iloprost in pulmonary arterial hypertension. Ann Pharmacother. 2005; 39:1265–1274. [PubMed: 15976392]

Bulte JW, Brooks RA, Moskowitz BM, Bryant LH Jr, Frank JA. Relaxometry and magnetometry of the MR contrast agent MION-46L. Magn Reson Med. 1999a; 42:379–384. [PubMed: 10440963]

Bulte JW, de Cuyper M, Despres D, Frank JA. Short- vs. long-circulating magnetoliposomes as bone marrow-seeking MR contrast agents. J Magn Reson Imaging. 1999b; 9:329–335. [PubMed: 10077033]

Cern A, Golbraikh A, Sedykh A, Tropsha A, Barenholz Y, Goldblum A. Quantitative structure-property relationship modeling of remote liposome loading of drugs. J Control Release. 2012; 160:147–157. [PubMed: 22154932]

Chattaraj SC. Treprostinil sodium Pharmacia. Curr Opin Investig Drugs. 2002; 3:582–586.

Chen XY, Dun JN, Miao QF, Zhang YJ. Fasudil hydrochloride hydrate, a Rho-kinase inhibitor, suppresses 5-hydroxytryptamine-induced pulmonary artery smooth muscle cell proliferation via JNK and ERK1/2 pathway. Pharmacology. 2009; 83:67–79. [PubMed: 19052484]

Chouly C, Pouliquen D, Lucet I, Jeune JJ, Jallet P. Development of superparamagnetic nanoparticles for MRI: effect of particle size, charge and surface nature on biodistribution. J Microencapsul. 1996; 13:245–255. [PubMed: 8860681]

Conhaim RL, Eaton A, Staub NC, Heath TD. Equivalent pore estimate for the alveolar-airway barrier in isolated dog lung. J Appl Physiol. 1988; 64:1134–1142. [PubMed: 2452819]

Duguet E, Vasseur S, Mornet S, Devoisselle JM. Magnetic nanoparticles and their applications in medicine. Nanomedicine. 2006; 1:157–168. [PubMed: 17716105]

Geiser M. Update on macrophage clearance of inhaled micro- and nanoparticles. J Aerosol Med Pulm Drug Deliv. 2010; 23:207–217. [PubMed: 20109124]

Gupta AK, Gupta M. Synthesis and surface engineering of iron oxide nanoparticles for biomedical applications. Biomaterials. 2005; 26:3995–4021. [PubMed: 15626447]

Gupta V, Ahsan F. Influence of PEI as a core modifying agent on PLGA microspheres of PGE(1), a pulmonary selective vasodilator. Int J Pharm. 2011; 413:51–62. [PubMed: 21530623]

Gupta V, Gupta N, Shaik IH, Mehvar R, McMurtry IF, Oka M, Nozik-Grayck E, Komatsu M, Ahsan F. Liposomal fasudil, a rho-kinase inhibitor, for prolonged pulmonary preferential vasodilation in pulmonary arterial hypertension. J Control Release. 2013; 167:189–199. [PubMed: 23353807]

Ishida T, Takanashi Y, Doi H, Yamamoto I, Kiwada H. Encapsulation of an antivasospastic drug, fasudil, into liposomes, and in vitro stability of the fasudil-loaded liposomes. Int J Pharm. 2002; 232:59–67. [PubMed: 11790490]

Jain TK, Richey J, Strand M, Leslie-Pelecky DL, Flask CA, Labhasetwar V. Magnetic nanoparticles with dual functional properties: drug delivery and magnetic resonance imaging. Biomaterials. 2008; 29:4012–4021. [PubMed: 18649936]

Jung CW, Jacobs P. Physical and chemical properties of superparamagnetic iron oxide MR contrast agents: ferumoxides, ferumoxtran, ferumoxsil. Magn Reson Imaging. 1995; 13:661–674. [PubMed: 8569441]

Kim SY, Lee YM. Taxol-loaded block copolymer nanospheres composed of methoxy poly(ethylene glycol) and poly(epsilon-caprolactone) as novel anticancer drug carriers. Biomaterials. 2001; 22:1697–1704. [PubMed: 11396872]

Kimura K, Ito M, Amano M, Chihara K, Fukata Y, Nakafuku M, Yamamori B, Feng J, Nakano T, Okawa K, Iwamatsu A, Kaibuchi K. Regulation of myosin phosphatase by Rho and Rho-associated kinase (Rho-kinase). Science. 1996; 273:245–248. [PubMed: 8662509]

Kreuter J. Nanoparticulate systems for brain delivery of drugs. Adv Drug Deliv Rev. 2001; 47:65–81. [PubMed: 11251246]

Laouini A, Jaafar-Maalej C, Limayem-Blouza I, Sfar S, Charcosset C, Fessi H. Preparation, Characterization and Applications of Liposomes: State of the Art. J Colloid Sci Biotechnol. 2012; 1:147–168.

Li F, Sun J, Zhu H, Wen X, Lin C, Shi D. Preparation and characterization novel polymer-coated magnetic nanoparticles as carriers for doxorubicin. Colloids Surf B Biointerfaces. 2011; 88:58–62. [PubMed: 21764271]

Lian T, Ho RJ. Trends and developments in liposome drug delivery systems. J Pharm Sci. 2001; 90:667–680. [PubMed: 11357170]

Liu AJ, Ling F, Wang D, Wang Q, Lu XD, Liu YL. Fasudil inhibits platelet-derived growth factor-induced human pulmonary artery smooth muscle cell proliferation by up-regulation of p27kip(1) via the ERK signal pathway. Chin Med J (Engl). 2011; 124:3098–3104. [PubMed: 22040563]

McLaughlin VV, McGoon MD. Pulmonary arterial hypertension. Circulation. 2006; 114:1417–1431. [PubMed: 17000921]

Medeiros SFS, Fessi AM, Elaissari H. Stimuli-responsive magnetic particles for biomedical applications. Int J Pharm. 2011; 403:139–161. [PubMed: 20951779]

Mitsumata T, Honda A, Kanazawa H, Kawai M. Magnetically Tunable Elasticity for Magnetic Hydrogels Consisting of Carrageenan and Carbonyl Iron Particles. J Phys Chem B. 2012

Mucke HA. Pulmonary arterial hypertension: on the way to a manageable disease. Curr Opin Investig Drugs. 2008; 9:957–962.

Nagaoka T, Fagan KA, Gebb SA, Morris KG, Suzuki T, Shimokawa H, McMurtry IF, Oka M. Inhaled Rho kinase inhibitors are potent and selective vasodilators in rat pulmonary hypertension. Am J Respir Crit Care Med. 2005; 171:494–499. [PubMed: 15563635]

Natarajan JV, Chattopadhyay S, Ang M, Darwitan A, Foo S, Zhen M, Koo M, Wong TT, Venkatraman SS. Sustained release of an anti-glaucoma drug: demonstration of efficacy of a liposomal formulation in the rabbit eye. PLoS One. 2011; 6:e24513. [PubMed: 21931735]

Oka M, Homma N, Taraseviciene-Stewart L, Morris KG, Kraskauskas D, Burns N, Voelkel NF, McMurtry IF. Rho kinase-mediated vasoconstriction is important in severe occlusive pulmonary arterial hypertension in rats. Circ Res. 2007; 100:923–929. [PubMed: 17332430]

Okon E, Pouliquen D, Okon P, Kovaleva ZV, Stepanova TP, Lavit SG, Kudryavtsev BN, Jallet P. Biodegradation of magnetite dextran nanoparticles in the rat. A histologic and biophysical study. Lab Invest. 1994; 71:895–903. [PubMed: 7807971]

Patel B, Gupta V, Ahsan F. PEG-PLGA based large porous particles for pulmonary delivery of a highly soluble drug, low molecular weight heparin. J Control Release. 2012; 162:310–320. [PubMed: 22800582]

Plank C. Nanomagnetosols: magnetism opens up new perspectives for targeted aerosol delivery to the lung. Trends Biotechnol. 2008; 26:59–63. [PubMed: 18191261]

Pradhan P, Giri J, Rieken F, Koch C, Mykhaylyk O, Doblinger M, Banerjee R, Bahadur D, Plank C. Targeted temperature sensitive magnetic liposomes for thermo-chemotherapy. J Control Release. 2010; 142:108–121. [PubMed: 19819275]

Reiss G, Hutten A. Magnetic nanoparticles: applications beyond data storage. Nat Mater. 2005; 4:725–726. [PubMed: 16195762]

Salomir R, Palussiere J, Fossheim SL, Rogstad A, Wiggen UN, Grenier N, Moonen CT. Local delivery of magnetic resonance (MR) contrast agent in kidney using thermosensitive liposomes and MR imaging-guided local hyperthermia: a feasibility study in vivo. J Magn Reson Imaging. 2005; 22:534–540. [PubMed: 16161081]

Schroeder U, Sommerfeld P, Ulrich S, Sabel BA. Nanoparticle technology for delivery of drugs across the blood-brain barrier. J Pharm Sci. 1998; 87:1305–1307. [PubMed: 9811481]

Shamim N, Hong L, Hidajat K, Uddin MS. Thermosensitive polymer (N-isopropylacrylamide) coated nanomagnetic particles: preparation and characterization. Colloids Surf B Biointerfaces. 2007; 55:51–58. [PubMed: 17178452]

Shinkai M, Le B, Honda H, Yoshikawa K, Shimizu K, Saga S, Wakabayashi T, Yoshida J, Kobayashi T. Targeting hyperthermia for renal cell carcinoma using human MN antigen-specific magnetoliposomes. Jpn J Cancer Res. 2001; 92:1138–1145. [PubMed: 11676866]

Shubayev VI, Pisanic TR 2nd, Jin S. Magnetic nanoparticles for theragnostics. Adv Drug Deliv Rev. 2009; 61:467–477. [PubMed: 19389434]

Uster PS, Allen TM, Daniel BE, Mendez CJ, Newman MS, Zhu GZ. Insertion of poly(ethylene glycol) derivatized phospholipid into pre-formed liposomes results in prolonged in vivo circulation time. FEBS Lett. 1996; 386:243–246. [PubMed: 8647291]

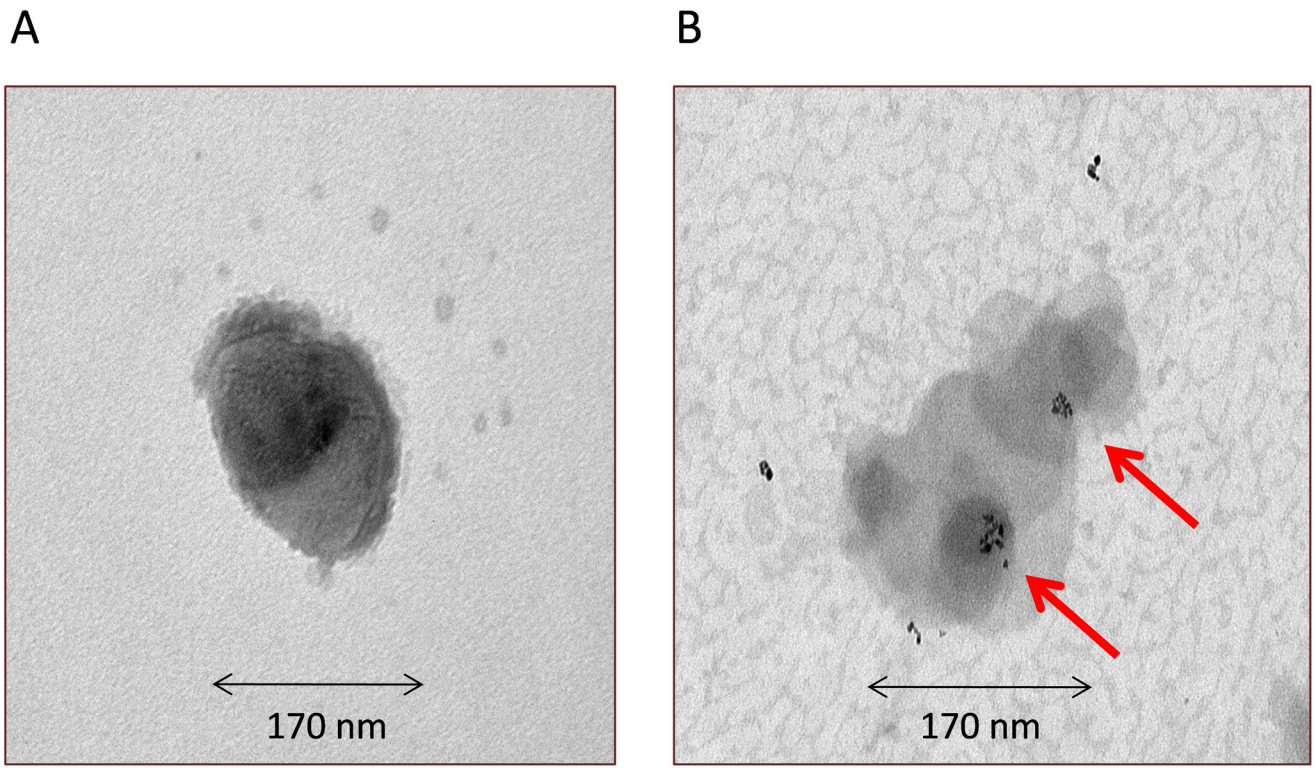

Fig. 1.

Transmission electron microscopic images of F-10 formulation: **(A)** intact magnetic liposome and **(B)** presence of magnetite (arrow) inside the liposome. Representative microphotograph of the dispersion of the formulation; six to seven pictures were taken and one of them is presented.

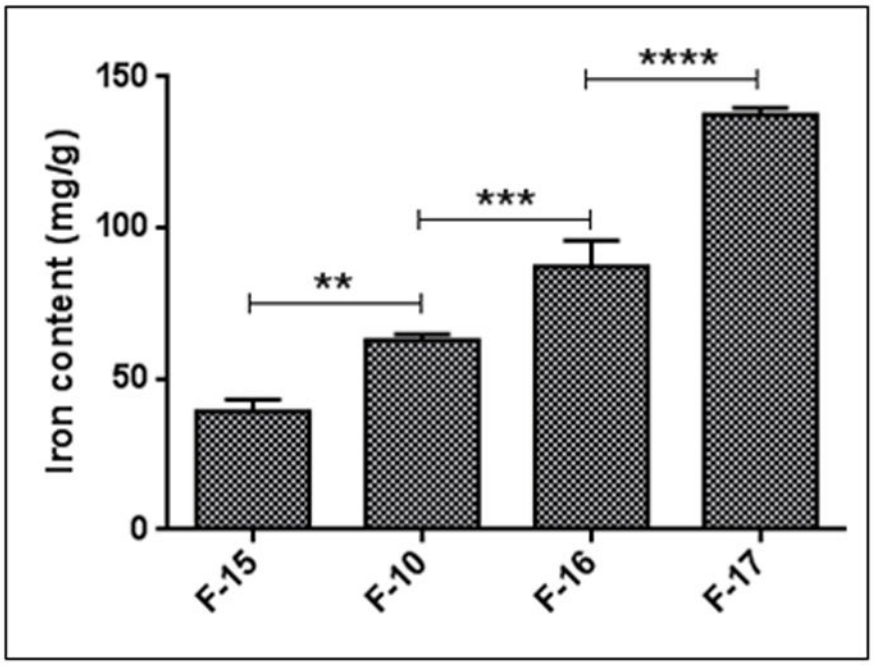

Fig. 2.

The effects of magnetite amount on iron content of F-15, F-10, F-16 and F-17 formulations (Please see Table 1). Data represent mean ± SD. n=3, $^{**}p<0.01$, $^{***}p<0.001$, $^{****}p<0.0001$.

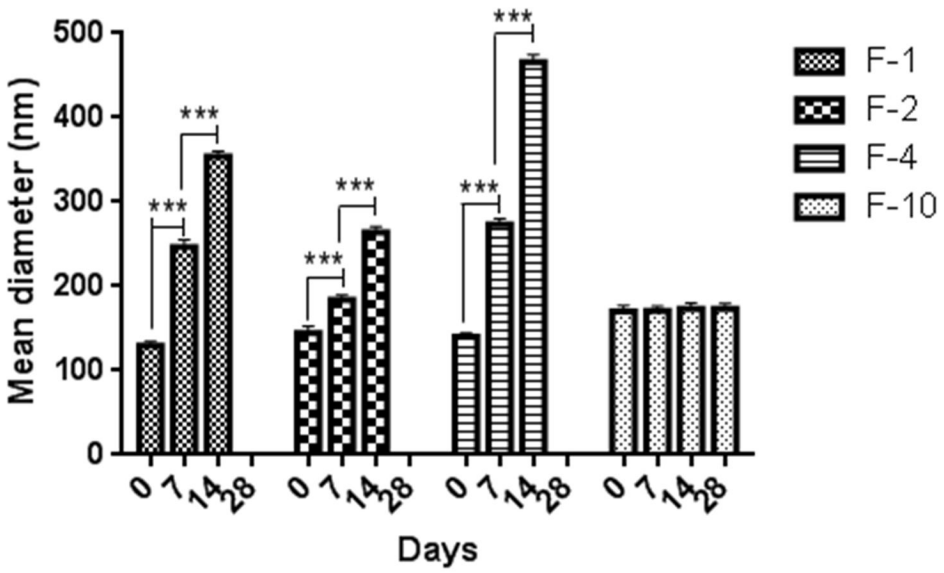

Fig. 3.

Physical stability of anionic (F-1), cationic (F-2), starch-coated non-pegylated (F-4) and pegylated (F-10) magnetic liposomes upon storage at 4°C. Data represent mean ± SD, n=3, ***p<0.001.

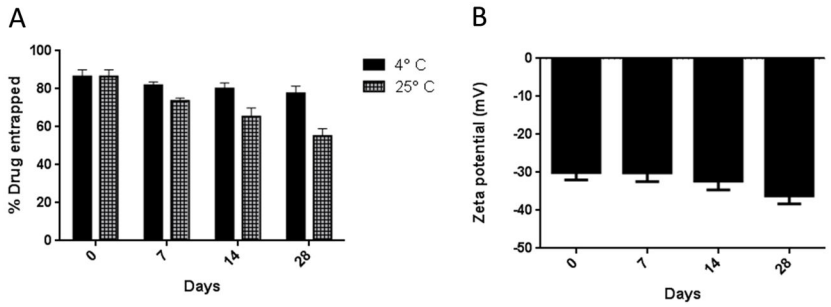

Fig. 4.

Physicochemical stability of starch-coated pegylated magnetic liposomes (F-10): **(A)** Entrapment efficiency and **(B)** Zeta potential. Data represent mean ± SD, n=3.

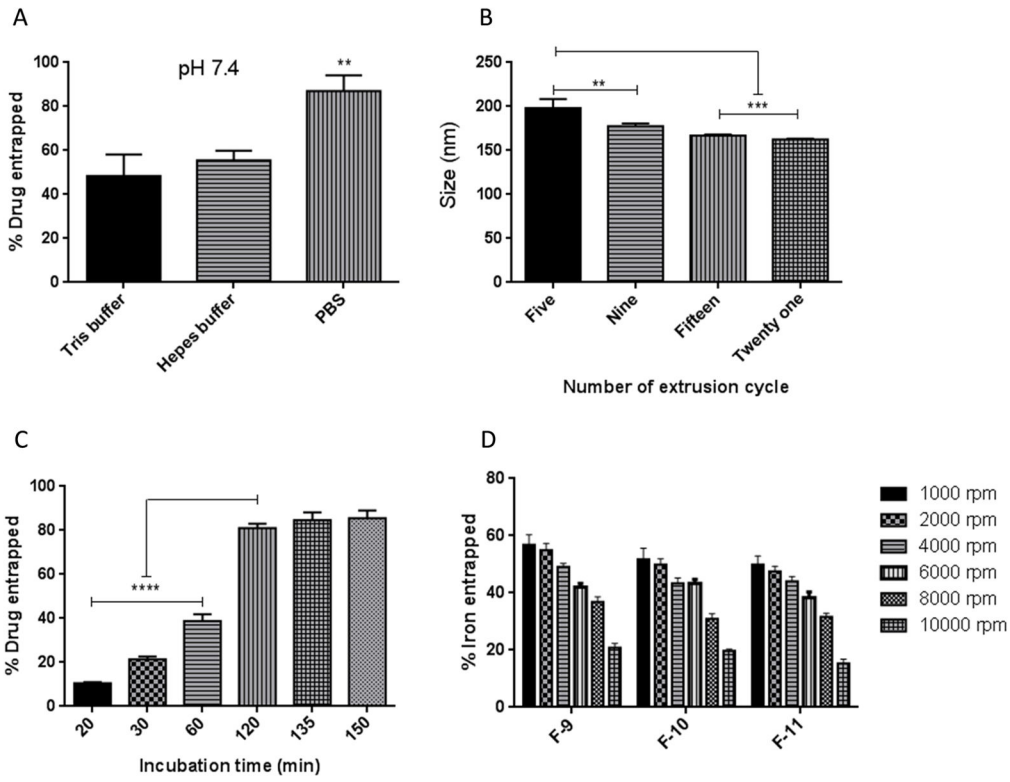

Fig. 5.

Optimization of process parameters: **(A)** buffer type, **(B)** number of extrusion cycle, **(C)** duration of incubation and **(D)** centrifugal speed for starch-coated pegylated liposomes. Data represent mean ± SD; n=3. ***p*<0.01, ****p*<0.001, *****p*<0.0001.

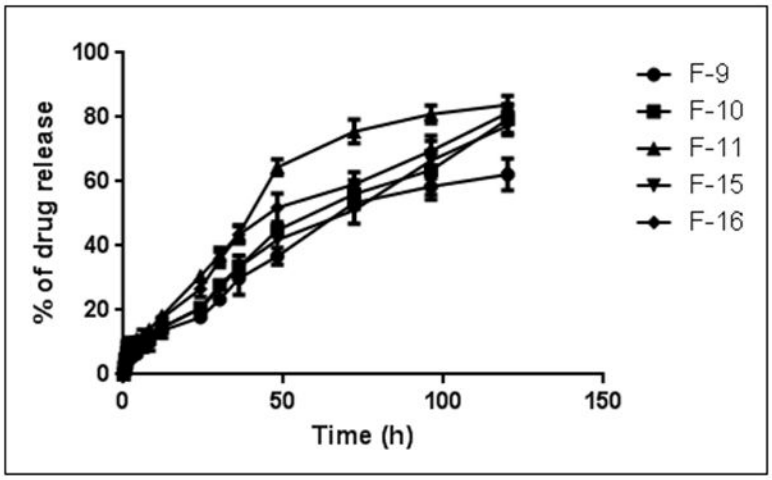

Fig. 6.

In vitro release profiles of fasudil-encapsulated magnetic liposomes in phosphate buffered saline at 37°C. Data represent mean ± SD, n=3.

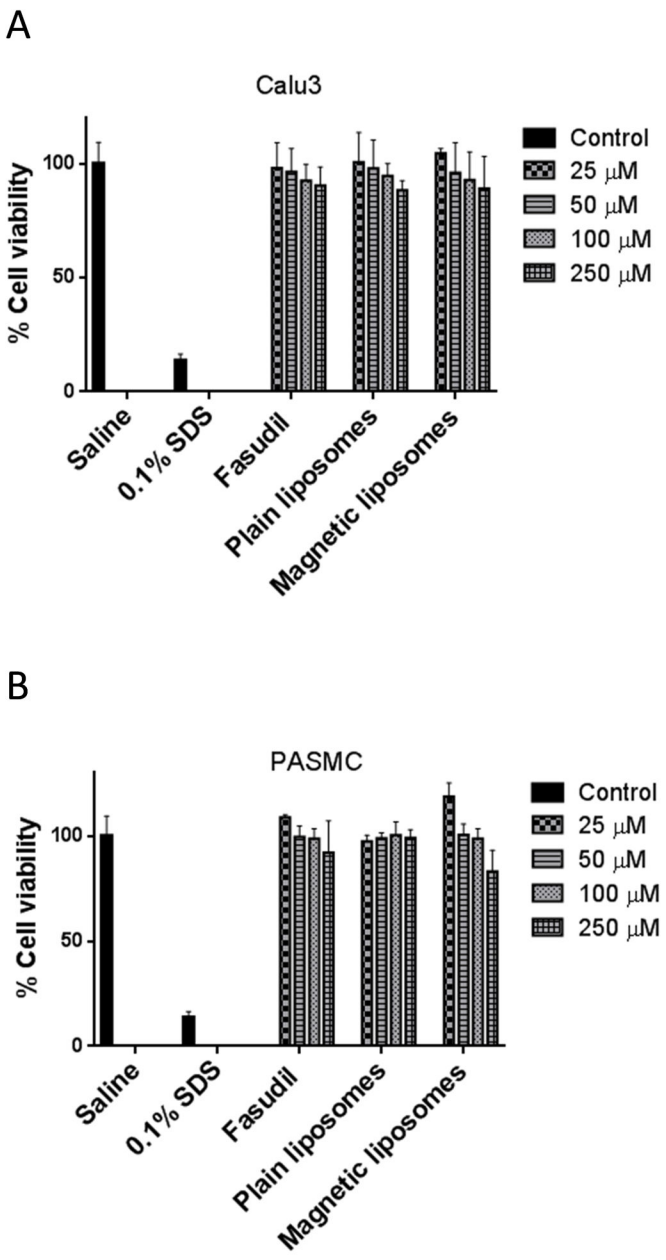

Fig. 7.

The safety of fasudil-encapsulated magnetic liposomes in **(A)** lung epithelial (Calu-3) and **(B)** pulmonary arterial smooth muscle cells upon acute exposure. Data represent mean ± SD; n=8.

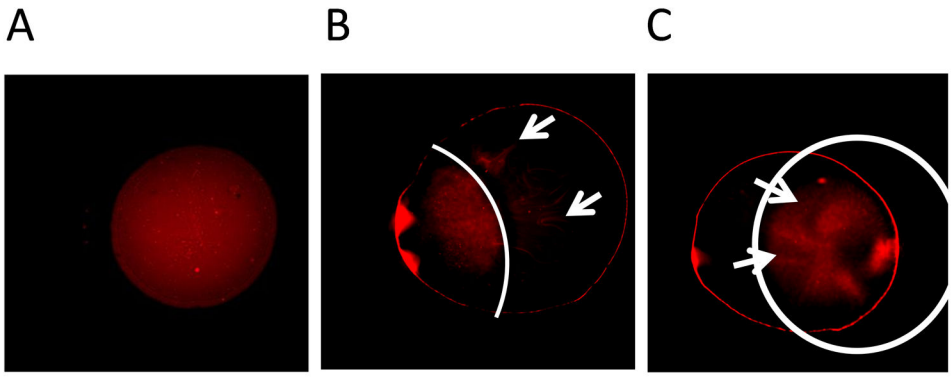

Fig. 8.

Magnetization of fasudil-encapsulated magnetic liposomes observed under the fluorescent microscope. **(A)** Homogeneous distribution of magnetic liposomes without magnetic field; **(B)** Spontaneous movement of liposomes towards the magnetic field; **(C)** Accumulation of magnetic liposomes in the applied magnetic area after 15 minutes of magnetization

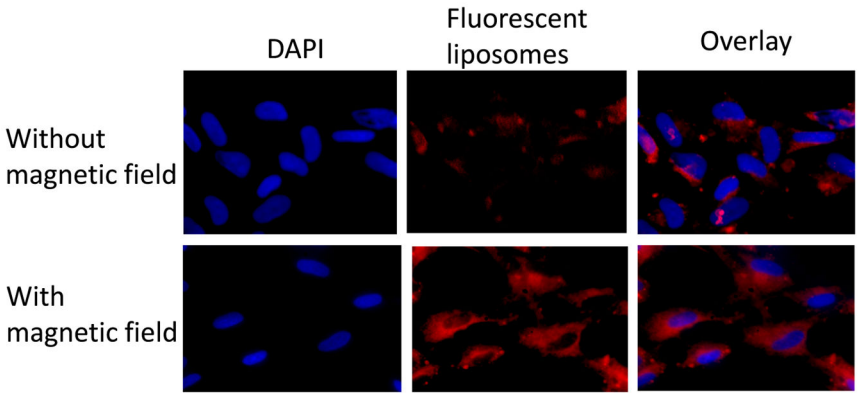

Fig. 9.

Representative fluorescence microscopic images showing the uptake of magnetic liposomes by the pulmonary arterial smooth muscle cells with and without the influence of external magnetic field. Left panel: cell nucleus stained with DAPI; middle panel-rhodamine B labeled liposomes; right panel-overlay. Top and bottom panels represent uptake in the absence and presence of magnetic field, respectively.

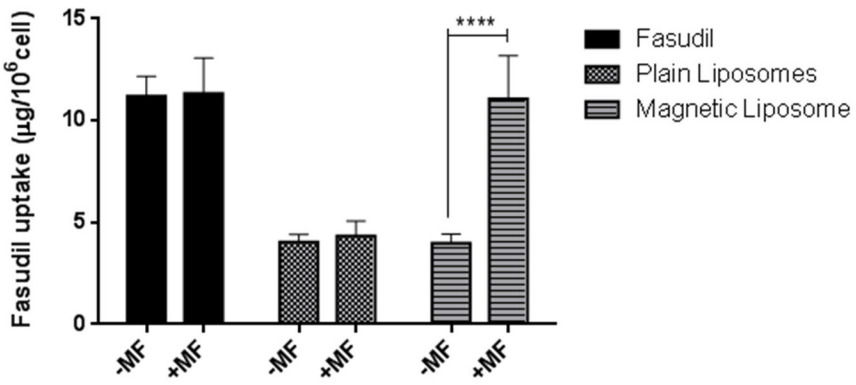

Fig. 10.

Quantitative analysis (HPLC) representing cellular uptake of magnetic liposomes with and without the influence of magnetic field. Data represent mean ± SD; n=3. ****$p<0.0001$.

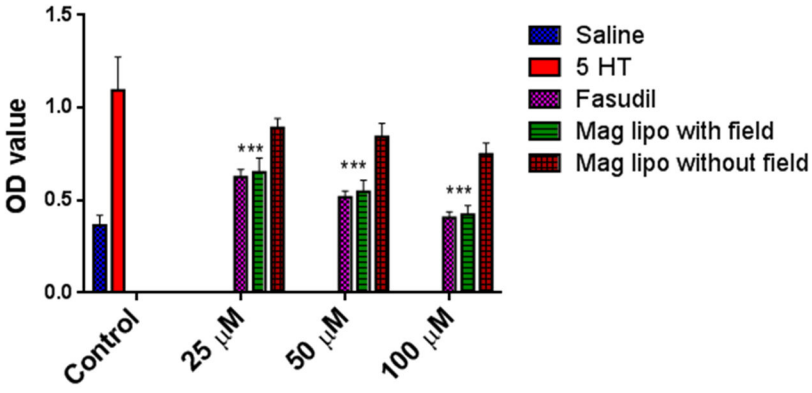

Fig 11.

Effect of fasudil-encapsulated magnetic liposomes on 5-HT induced PASMC-proliferation with and without the influence of applied magnetic field. Data represent mean ± SD; n=3. ****p<0.0001.

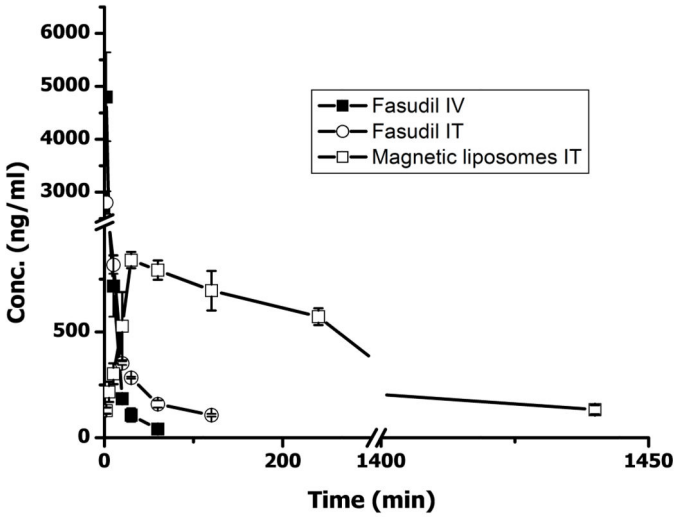

Formulation	C_{max} (ng/ml)	$t_{1/2}$ (min)	$AUC_{0\text{-}inf}$ (µg.min/ml)
Plain Fasudil IV	4801 ± 841	19 ± 4.8	39.9 ± 6.06
Plain Fasudil IT	2801 ± 211	35 ± 5.1	39.1 ± 2.90
Mag-liposome	840 ± 35	523 ± 31	559.3 ± 2.90

Fig 12.

In vivo absorption profile of fasudil following intravenous and intratracheal administration of plain fasudil and fasudil-encapsulated magnetic liposomes. Data represent mean ± SD; n=4.

Table 1

Composition and physicochemical parameters of the formulations

Formulation*	Lipid Composition	Lipid molar ratio	Lipid Quantity μmol	Magnetite Type	Magnetite Amount (mg)	Particle Size (nm)	PDI	Zeta Potential (mV)	Entrapment Efficiency (%)
F-1	DPPC: CH	70:30	50	Anionic	5	129.67±4.04	0.15±0.007	−40.4±1.22	4.5±0.5
F-2				Cationic		143±3.22	0.14±0.02	+52.2±2.94	5.5±0.5
F-3	DPPC: CH	60:40	50	Starch coated	5	119.1±2.021	0.34±0.05	−22.5±2.57	66.5±4.5
F-4		70:30				145±2.116	0.23±0.01	−17.3±3.6	62.5±5.5
F-5		80:20				199.8±2.183	0.14±0.01	−6.03±0.94	53±4.1
F-6	DPPC: CH: DSPE-Peg_{2000}	60:40:5	25	Starch coated	5	158.8±2.5	0.09±0.002	−31.4±0.78	59.1±5.05
F-7		70:30:5				163.8±2.35	0.08±0.22	−28.9±0.99	55±3.8
F-8		80:20:5				169.8±1.88	0.11±0.05	−28.6±0.79	51.5±2.9
F-9	DPPC: CH: DSPE-Peg_{2000}	60:40:5	50	Starch coated	5	164.83±4.21	0.12±0.01	−30.3±0.99	91.1±4.1
F-10		70:30:5				170.8±1.93	0.09±0.01	−34.8±0.26	85.5±3.5
F-11		80:20:5				172.9±0.67	0.09±0.01	−33.9±1.29	74.2±4.8
F-12	DPPC: CH: DSPE-Peg_{2000}	60:40:5	75	Starch coated	5	178.9±2.011	0.09±0.01	−28.9±0.79	92.5±4.9
F-13		70:30:5				175.7±3.84	0.09±0.04	−27.8±1.19	86.7±4.6
F-14		80:20:5				180.9±2.58	0.09±0.01	−26.9±1.04	81.5±3.1
F-15	DPPC: CH: DSPE-Peg_{2000}	70:30:5	50	Starch coated	2.5	147.11±3.01	0.96±0.01	−14.9±2.4	88.1±3.8
F-16					10	174.2±1.82	0.12±0.01	−26.2±6.99	76.8±4.9
F-17					20	178.2±1.21	0.09±0.02	−30.03±2.94	54.03±8.03
F-18	DPPC: CH: DSPE-Peg_{2000}	70:30:5	50	-	-	130.4±3.98	0.05±0.04	−9.58±1.74	88±4.3

*F-1 and F-2 were prepared by passive loading but F-3 to F-18 were prepare by active loading

Table 2

Nebulization stability of the Magnetic Nanoparticles

Nebulization	Particle size (nm)	Zeta Potential (mV)	Entrapment Efficiency (%)
Before	166 ± 2.34	−30.03 ± 2.94	81.51 ± 3.33
After	172 ± 2.80	−28.6 ± 2.5	81.40 ± 2.25